

Tissue- and Cell-Type-Specific Genetic Regulation of CTBPI in Breast Cancer: Integrative Analyses with Exploratory Single-Cell and Imaging Data

Minping Hong¹, XiaoWen Huang¹, Qin Xu¹, Zhenyi Ma^{1,*}, Keng Ling^{2,*}

¹Radiology Department, Jiaxing Hospital of Traditional Chinese Medicine, Jiaxing, Zhejiang, 314000, People's Republic of China; ²Clinical Laboratory, Jiaxing Maternity and Children Health Care Hospital, Jiaxing, Zhejiang, 314000, People's Republic of China

*These authors contributed equally to this work

Correspondence: Keng Ling, Clinical Laboratory, Jiaxing Maternity and Children Health Care Hospital, Jiaxing, Zhejiang, 314000, People's Republic of China, Email 450620239@qq.com; Zhenyi Ma, Radiology department, Jiaxing Hospital of Traditional Chinese Medicine, No. 1501 Zhongshan East Road, Nanhu District, Jiaxing, Zhejiang, 314000, People's Republic of China, Email 172702978@qq.com

Background: CTBPI, an NADH-dependent transcriptional co-repressor subject to succinylation, may orchestrate both systemic and cell-type-specific effects on tumor development.

Methods: This integrative study represents a novel approach, combining genetic regulation, single-cell expression quantitative trait loci (eQTLs), and imaging radiomics to investigate CTBPI in breast cancer. We integrated tissue-relevant eQTLs with breast cancer GWAS to evaluate genetically proxied associations for CTBPI. We further explored cell-type-dependent effects using single-cell eQTL resources and examined expression, survival, and imaging correlations as hypothesis-generating evidence.

Results: Tissue-focused analyses suggested an inverse association between CTBPI expression and breast cancer risk, with consistent directions observed in expression and survival datasets. Single-cell explorations indicated potential cell-type-specific regulation. Imaging correlations with MRI-derived features were modest and exploratory.

Conclusion: Our results prioritise CTBPI as a context-dependent, tissue- and cell-type-specific candidate in breast cancer. The observational and exploratory components warrant validation in larger cohorts and functional assays. To our knowledge, this is the first integrative study combining GWAS, single-cell eQTL and MRI radiomics to prioritize CTBPI in breast cancer.

Keywords: CTBPI, breast cancer, single-cell RNA-seq, single-cell eQTL, Mendelian randomization, DCE-MRI radiomics, cell-cell communication

Introduction

Breast cancer remains one of the most prevalent and lethal malignancies among women globally, with rising incidence and substantial mortality rates presenting a significant challenge to public health worldwide.^{1–3} Despite advancements in early diagnosis and therapeutic interventions, clinical outcomes remain unpredictable, primarily due to tumor heterogeneity, treatment resistance, and immune evasion mechanisms.^{4,5} These challenges underscore the critical need to identify novel, reliable biomarkers for risk prediction, prognostic assessment, and personalized therapeutic strategies.

Metabolic reprogramming is increasingly recognized as a hallmark of cancer initiation and progression.^{6,7} Among post-translational modifications (PTMs) involved in regulating cancer metabolism and immune surveillance, lysine succinylation has emerged as a key regulator of tumor biology.⁸ This modification alters protein structure and function, thereby modulating gene expression, metabolic flux, and immune signaling.^{9,10}

While the role of succinylation in tumor biology has been increasingly acknowledged, its specific mechanisms in breast cancer remain underexplored, particularly in relation to its involvement in the immune microenvironment and imaging characteristics. This gap in knowledge limits the development of targeted interventions and prognostic tools. Therefore, constructing a comprehensive breast cancer prognostic model that integrates metabolic information, immune response, and

imaging features based on succinylation is of paramount clinical importance. Beyond its metabolic regulation, CTBP1 has been extensively implicated in cancer biology as a transcriptional corepressor promoting tumor proliferation, epithelial–mesenchymal transition (EMT), and metastasis through multiple pathways, such as the CDH1 repression axis and TGF- β signaling.^{11–15} In breast and other cancers, CTBP1 also interacts with metabolic and chromatin modifiers, thereby linking redox homeostasis to oncogenic transcriptional programs.^{11,12} These findings support the rationale to explore both the tissue- and cell-specific regulatory mechanisms of CTBP1 in breast cancer.

This study aimed to prioritise CTBP1 in breast cancer by integrating tissue-relevant genetic instruments with disease GWAS and by exploring cell-type-specific signals. We further complemented these analyses with expression, survival, and radiomics correlations as hypothesis-generating evidence rather than definitive biomarkers. CTBP1 is of particular interest in breast cancer because it bridges cellular metabolism with transcriptional control and immune regulation. Prior studies have shown that CTBP1 represses E-cadherin and modulates redox-sensitive transcription factors, influencing both tumor invasiveness and immune evasion. However, its regulation appears context-dependent and may differ across tissue or cell types. To address these gaps, our study integrates genetic, single-cell, and MRI radiomics data to systematically characterize CTBP1 regulation across multiple biological levels.

Materials and Methods

Selection of Hotspot Genes

This study collected a total of 19 Succinylation-related genes.^{9,10,16–18} A detailed list of the genes is provided in [Supplemental Table S1](#). The overall workflow is summarized in [Supplementary Figure S1](#).

eQTL Dataset

The eQTL data for all genes in this study were obtained from the eQTLGen database (website: <https://www.eqtlgen.org/cis-eqtls.html>), and all data correspond to cis-eQTLs derived from blood samples. Instrumental SNPs were defined as genome-wide significant ($P < 5 \times 10^{-8}$) and LD-independent (clumping window 10 Mb, $r^2 < 0.1$). After filtering, cis-eQTL information remained for 15,695 genes. Intersecting this set with the 19 succinylation-related genes yielded 16 candidates.

Breast Cancer Outcome Dataset

Breast cancer outcome data were obtained from the FinnGen consortium (release R11; <https://www.finnngen.fi/en>). The analytic cohort comprised 222,080 participants of European ancestry (20,586 cases; 201,494 controls).

Two-Sample MR Framework

We conducted two-sample MR using the TwoSampleMR R package (v4.3.1). Cis-eQTL proxies for succinylation-related genes served as exposures, and breast cancer status was the outcome. To limit weak-instrument bias, variants with F-statistics < 10 were removed. The main estimator was inverse-variance weighting (IVW); exposures lacking computable IVW effects were omitted. Horizontal pleiotropy was evaluated with the MR-Egger intercept, heterogeneity with Cochran's Q, and robustness with leave-one-out analyses.

SMR Framework and Colocalization Tests

Summary-data-based Mendelian randomization (SMR) was used to integrate GWAS summary statistics with GTEx Breast_Mammary_Tissue eQTLs, testing whether variation in gene expression is associated with the trait via a shared causal variant. Analyses were run with the official SMR software v1.3.1 (<https://yanglab.westlake.edu.cn/software/smr/#Overview>) using default settings. To distinguish pleiotropy from linkage, we applied the HEIDI test; failure to reject the HEIDI null (no heterogeneity) supports compatibility with a single variant underlying both the expression and trait signals.

Differential Expression Analysis and Survival Analysis

Gene expression analysis was performed using the Breast Cancer Gene-Expression Miner v5.2 website (<https://bcgenex.unicancer.fr/BC-GEM/GEM-requete.php>),¹⁹ comparing cancer tissue (743 cases) with adjacent normal tissue (92 cases) and healthy control tissue (89 cases). Survival analysis was performed using the Kaplan-Meier Plotter website (<https://kmplot.com/analysis/>).²⁰ ELISA peripheral blood samples were collected from breast cancer patients (n=40) and normal controls (n=40) at Jiaxing Hospital of Traditional Chinese Medical (Jiayitong Medical Ethics Review 2023 Research No. 095–1). Ethical approval was obtained from the hospital's ethics committee, and informed consent was obtained from all participants.

Serum CTBP1 concentrations were quantified using a commercially available human CTBP1 ELISA kit. Measurements were performed in duplicate according to the manufacturer's instructions. Optical density was read at 450 nm, and concentration values were interpolated from standard curves. Because the GWAS datasets are predominantly of European ancestry, whereas the ELISA validation cohort comprises Chinese participants, potential population stratification bias cannot be fully excluded.

Single-Cell Mendelian Randomization Analysis

Single-cell eQTL data were from the OneK1K (<https://onek1k.org/>).^{21,22} The following SNP selection criteria were applied: p-value < 0.05, clumping window: 10,0 kb, $r^2 < 0.3$, resulting in 14 cell-related data points. This component should be regarded as exploratory and hypothesis-generating rather than confirmatory.

DCE-MRI Radiomics Correlation

Dynamic contrast-enhanced (DCE) MRI scans were sourced from the TCGA imaging archive. Tumor volumes of interest (VOIs) on peak-phase images were first segmented with the U²-Net model and then manually refined by two radiologists (M.P.H., J.Y.W). To harmonize inter-scanner variation, images were resampled to isotropic 1×1×1 mm³ using linear interpolation. A 15-pixel 3D margin was appended around the tumor during segmentation, followed by intensity histogram equalization stratified by field strength. Radiomic features—shape, first-order, texture, wavelet, exponential, and square-filtered—were extracted with PyRadiomics v3.0.1. To assess repeatability, segmentation and extraction were repeated after two months in 50 cases to compute intraclass correlation coefficients (ICC). Pearson correlations were then calculated between hub-gene expression and the radiomic features. Correlation analyses between radiomic features and CTBP1 expression were adjusted for testing using the p_value (p < 0.05).

Generation of Single-Cell Suspensions From Human Specimens

Human tissue from healthy donors and patients was handled on ice in sterile, RNase-free dishes preloaded with calcium- and magnesium-free 1× PBS. Specimens were transferred, minced into ~0.5 mm² fragments, and repeatedly rinsed with 1× PBS to remove non-target material (eg, blood clots and adipose layers). Single-cell dissociation was performed by incubating the fragments in an enzyme cocktail (0.35% collagenase IV, 2 mg/mL papain, 120 U/mL DNase I) at 37 °C with shaking at 100 rpm for 20 min. Digestion was quenched with 1× PBS containing 10% (v/v) fetal bovine serum (FBS). The suspension was gently triturated 5–10 times using a Pasteur pipette, passed through stacked 70- and 30-μm strainers, and pelleted by centrifugation (300 g, 5 min, 4 °C). Cells were resuspended in 100 μL 1× PBS (0.04% BSA) and treated with 1 mL of 1× red blood cell lysis buffer (MACS 130–094-183, 10× stock) for 2–10 min at room temperature or on ice. After centrifugation (300 g, 5 min, RT), the supernatant was discarded and the pellet was incubated with 100 μL Dead Cell Removal MicroBeads (MACS 130–090-101) and processed using the Miltenyi[®] Dead Cell Removal Kit (MACS 130–090-101). The cells were washed twice in 1× PBS (0.04% BSA) with brief spins (300 g, 3 min, 4 °C) and finally resuspended in 50 μL 1× PBS (0.04% BSA). Viability was assessed by trypan blue exclusion, and preparations with >85% viable cells were retained. Cell counts were obtained on a Countess II Automated Cell Counter and adjusted to 700–1200 cells/μL.

Single-Cell Capture and Library Preparation (DNBelab C-TaiM 4; DNBSEQ-T7 Sequencing)

Single-cell suspensions were processed on the DNBelab C-TaiM 4 platform to target capture of ~8,000 cells, following the manufacturer's guidance aligned with the 10x Genomics Chromium Single Cell 3' Kit (v3). cDNA amplification and library preparation proceeded per the standard workflow.²³ Libraries were sequenced on a DNBSEQ-T7 (paired-end, 150 bp) with a minimum yield of 100 G.

Single-Cell RNA-Seq Data Preprocessing and Integration

Raw UMI count matrices from six scRNA-seq libraries (control.1–3, treat.4–6) were imported into Seurat objects (min.cells = 3, min.features = 200). Doublets were detected and removed with DoubletFinder v1.2.2 (default parameters). After doublet removal, cells were further filtered to retain only those with >50 detected genes (nFeature_RNA > 50) and <5% mitochondrial content (percent.mt < 5), and normalized by log-transformation (NormalizeData, scale.factor = 10,000). The top 1,500 variable genes per sample were identified using vst (FindVariableFeatures, nfeatures = 1500).

Batch correction and dimensionality reduction were performed via Seurat's integration workflow: anchors were identified across the six samples (FindIntegrationAnchors) and integrated into a single dataset (IntegrateData). To further remove residual batch effects, Harmony (RunHarmony on "orig.ident") was applied to the integrated PCA space. The data were scaled (ScaleData) and principal component analysis was run on the 1,500 most variable genes (RunPCA, npcs = 20). JackStraw analysis (JackStraw & ScoreJackStraw) was used to assess PC significance.

Clustering and Marker Identification

A shared-nearest neighbor graph was constructed on the first 20 Harmony-corrected PCs (FindNeighbors), and cells were clustered at resolution = 0.6 (FindClusters). UMAP embedding (RunUMAP, dims = 1:20) was used for visualization. Cluster marker genes were identified with FindAllMarkers (only.pos = FALSE, min.pct = 0.25, logfc.threshold = 1), and markers with $|\text{avg_log2FC}| > 1$ and adjusted $p < 0.05$ were retained.

Cell-Type Annotation and Differential Analysis

Cluster identities were annotated using SingleR v1.2.4 against the BlueprintEncode human reference (BlueprintEncode_bpe.se_human), and Seurat was used to rename clusters accordingly. To compare pCR versus non-pCR within each annotated cell type, we defined sample-cellType groups and ran FindMarkers, retaining genes with $|\text{avg_log2FC}| > 1$ and adjusted $p < 0.05$. Continuous QC and all downstream analyses were performed in R using Seurat v4.0.0 and Harmony v1.0.

Subclustering of CD8 Cell Types

CD8⁺ T cells were first subset from the globally integrated atlas. These CD8⁺ cells were then re-integrated to enable fine-grained subclustering. After integration, gene expression values were standardized to unit variance, and scaling, dimensionality reduction, and clustering were carried out as described above.

Developmental Trajectory Inference

Monocle 2 infers cell trajectories with reversed graph embedding, enabling unsupervised modeling of branched fate decisions. We applied Monocle 2 to construct pseudotime trajectories.

Cell-Cell Interactions Analysis by CellPhoneDB

CellPhoneDB is a curated resource cataloging ligands, receptors, and their interactions, with subunit-level annotations to represent heteromeric complexes. We used CellPhoneDB (v2.1.4) to infer intercellular communication. Receptor–ligand pairs were retrieved from the official downloads page (<https://www.cellphonedb.org/downloads>), and interactions with $p < 0.05$ were considered significant.

Statistical Methods

All analyses were conducted in R (version 4.3.1; <https://www.r-project.org/>). Statistical significance was defined as $p < 0.05$.

Results

Potential Causal Relationship Between CTBP1 and Breast Cancer

We utilized the IEU OpenGWAS eQTLs dataset for discovery. As shown in the IVW-MR analysis ([Supplemental Table S2](#)), CTBP1 eQTLs from this dataset were causally linked to breast cancer and associated with a significant reduction in breast cancer risk (OR = 0.95, 95% CI = 0.908–0.999, $p = 0.04$) ([Figure 1A and B](#)).

Additionally, the SMR analysis identified CTBP1 as a potential protective gene linked to a favorable prognosis in breast cancer (SMR $p = 0.02$, OR = 0.93, p HEIDI > 0.05) ([Figure 1C](#)) ([Supplemental Table S3](#)). The survival analysis further supported that CTBP1 could be a potential protective factor for breast cancer ([Figure 1D](#)). This was corroborated by public database analyses, which indicated differential expression of CTBP1 between breast cancer patients and normal controls ([Figure 1E](#)). The clinical ELISA results, showing the difference in CTBP1 protein expression between breast cancer patients and normal controls ([Figure 1F](#)).

sceQTL Analysis with CTBP1

[Figure 2](#) presents the results of the single-cell Mendelian randomization (MR) analysis performed on tumor samples from breast cancer patients. The analysis reveals that CTBP1 expression in CD8+ T-cells is significantly associated with immune-related features, such as S100B expression. We observed a positive correlation between CTBP1 and S100B in these cells (odds ratio [OR] = 1.25, 95% confidence interval [CI] = 1.108–1.414, $p < 0.01$), suggesting that CTBP1 may

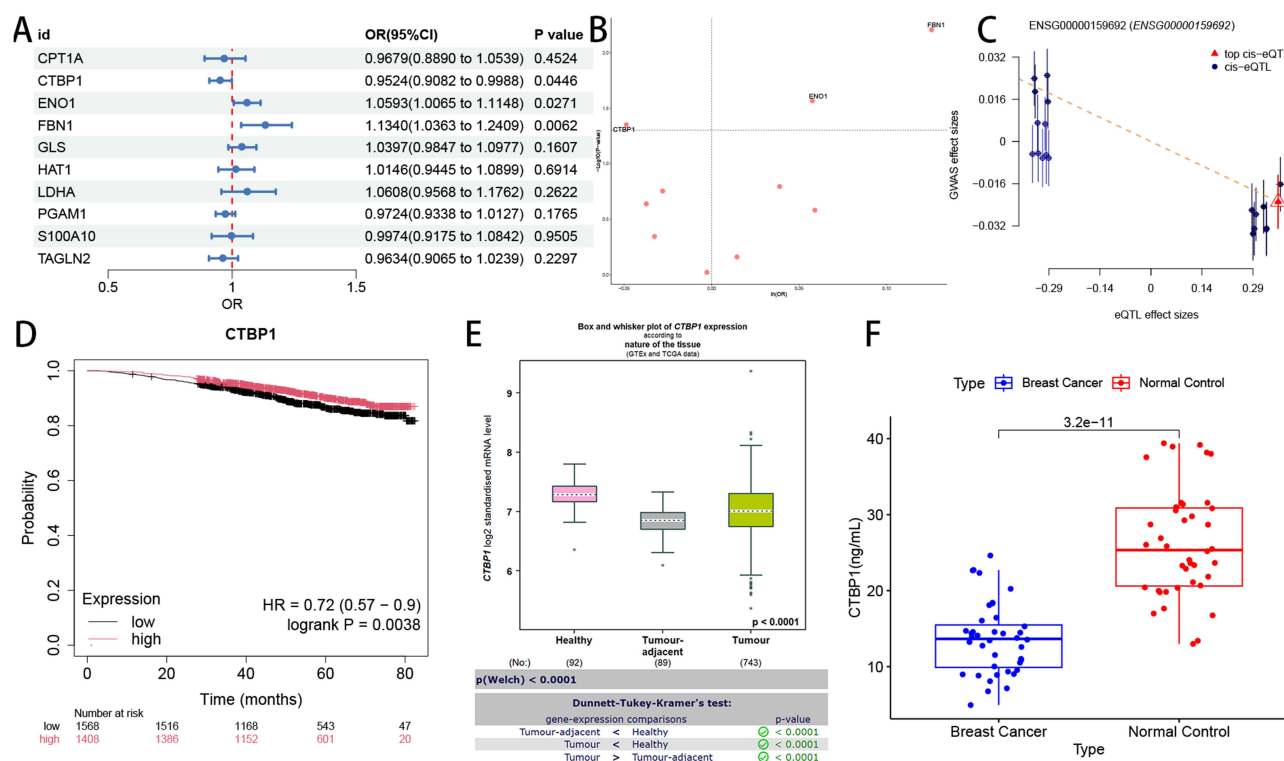


Figure 1 CTBP1 and Breast Cancer: Causal, Prognostic and Expression Patterns. Healthy controls were selected from the TCGA and GTEx dataset, with no history of breast cancer or related conditions. (A): Forest plot of IVW - MR analysis from the IEU OpenGWAS dataset, showing the causal association between eQTL and breast cancer. (B): Scatter plot corresponding to A, assisting in presenting the causal association between eQTL and breast cancer. (C): Result based on SMR analysis, indicating that CTBP1 is a potential protective gene for breast cancer prognosis. (D): Survival analysis plot, confirming the potential protective role of CTBP1 in breast cancer. (E): Box plot based on GTEx and TCGA data, showing the mRNA expression level of CTBP1 in different tissues ($p < 0.0001$). (F): Box plot of clinical ELISA results, showing the difference in CTBP1 protein expression between breast cancer patients and normal controls.

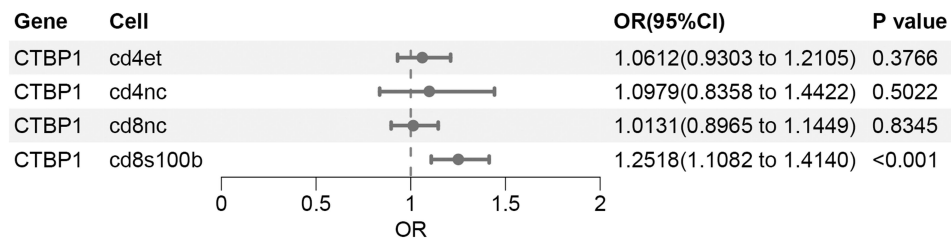


Figure 2 sceQTL analysis with CTBP1: Forest plot of IVW - MR analysis from the OneKIK dataset, showing the causal association between sceQTL and breast cancer.

regulate immune responses within the tumor microenvironment. This finding underscores the potential of single-cell MR analysis to identify cell-type-specific regulatory mechanisms in breast cancer, providing a deeper understanding of the immune interactions within the tumor.

Radiomics Correlations with CTBP1

A total of 944 radiomic features were extracted from each VOI in the MRI images. Pearson correlation analysis revealed that CTBP1 expression was positively associated with the wavelet-based feature HHH_gldm_LargeDependenceHighGrayLevelEmphasis (Cor = 0.28, $p < 0.05$) but negatively correlated with HHH_gldm_SmallDependenceLowGrayLevelEmphasis (Cor = -0.27, $p < 0.05$) (Figure 3A)(Supplemental Table S4). Two typical samples are presented for demonstration (Figure 3B and C). These findings suggest that CTBP1 may be associated with specific radiomic features that reflect tumor heterogeneity and could potentially serve as an imaging biomarker for breast cancer prognosis.

The Immune Microenvironment of BRCA

We first performed global clustering of single-cell data from six breast tissue samples (3 controls and 3 tumors with higher malignancy) and identified eight major cell populations in the UMAP embedding, including epithelial cells, CD8⁺T cells, CD4⁺T cells, macrophages, and others (Figure 4A and B). CellChat communication analysis indicated that this subset interacts most actively with epithelial cells, macrophages, and CD4⁺T cells (Figure 4C). We then reclustered all CD8⁺T cells and delineated six functionally distinct subtypes: Naive CD8 T, Effector Memory CD8 T, Tissue-resident Memory CD8 T, Central Memory CD8T, Exhausted CD8T, and the CD8⁺S100B⁺T cell of interest (Figure 4D and E). The Monocle-inferred pseudotime trajectory shows that the CD8⁺S100B⁺T cells (red) are positioned at the bottom left of the trajectory plot (Figure 4F), suggesting that this subset may reside in an early activation state or on a distinct differentiation branch, with high functional plasticity. Sample-wise UMAP plots revealed that this subset is consistently present across all samples and is slightly enriched in tumor tissues (Figure 4G). Finally, overlaying CTBP1 expression on the UMAP highlighted its concentrated expression within CD8⁺S100B⁺T cells, with higher levels observed in tumor samples compared to controls, supporting its potential functional role in the tumor immune microenvironment (Figure 4H).

Discussion

In summary, our integrative analyses reveal a context-dependent role for CTBP1 in breast cancer. Using tissue-relevant genetic instruments, both Mendelian randomization (IVW-MR OR = 0.95, $p = 0.04$) and SMR (SMR OR = 0.93, $p = 0.02$) indicated an inverse genetically-proxied association between whole-blood CTBP1 expression and breast cancer risk, consistent with GTEx and TCGA transcriptomic patterns, as well as our ELISA data. In contrast, exploratory single-cell eQTL analyses identified a positive association between CTBP1 expression and immune-related features within the CD8⁺S100B⁺T-cell subset (OR = 1.25, $p < 0.01$). Additionally, radiomics analysis showed modest correlations between CTBP1 expression and MRI-derived texture-dependence features. Further, CellChat analysis suggested enriched cell-cell communication between CD8⁺S100B⁺T cells, epithelial cells, macrophages, and CD4⁺T cells, indicating a potential role for CTBP1 in immune regulation within the tumor microenvironment.

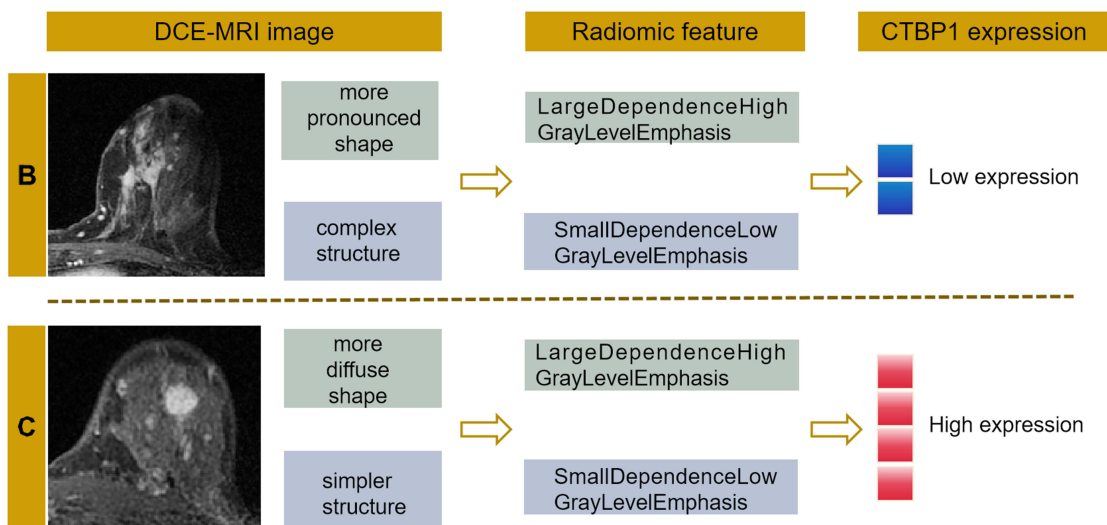
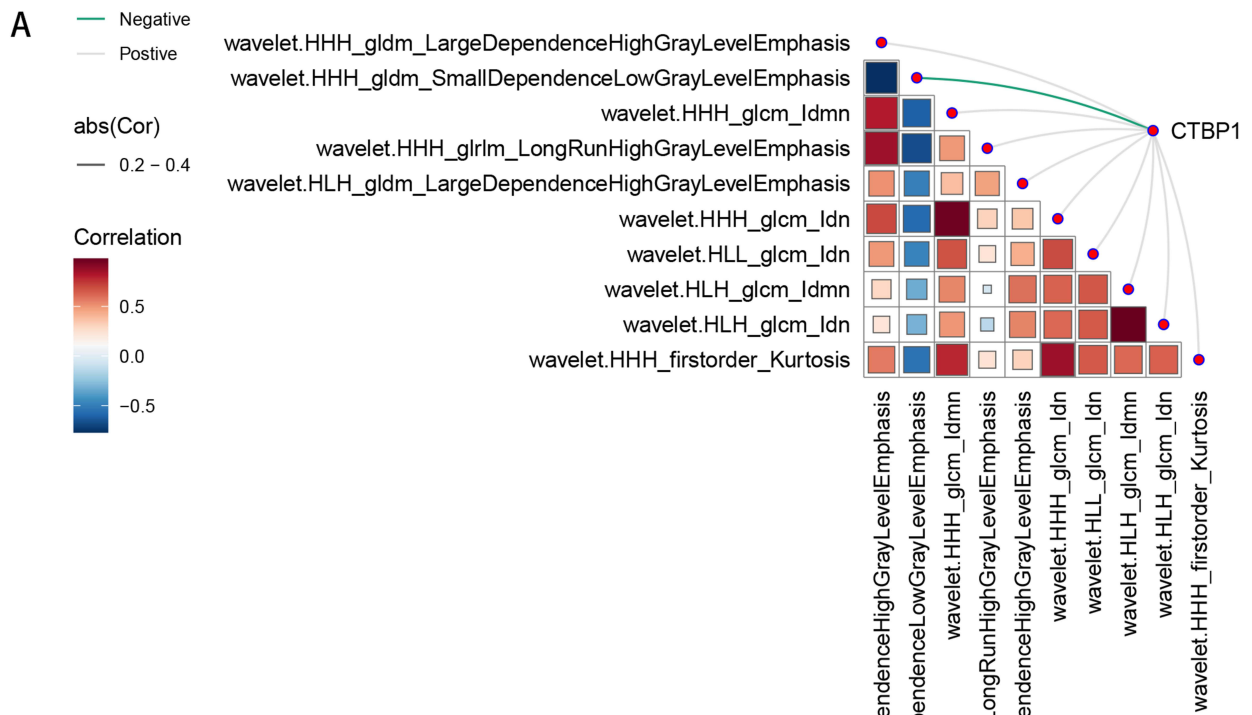


Figure 3 Radiomics Correlations with CTBP1, Representative cases illustrating the micro-macro relationship among imaging features and CTBP1 expression. **(A):** Top 10 radiomic features correlated with CTBP1 expression. **(B):** Case TCGA-BH-A0B5 (low CTBP1 expression). **(C):** Case TCGA-BH-A0BQ (high CTBP1 expression).

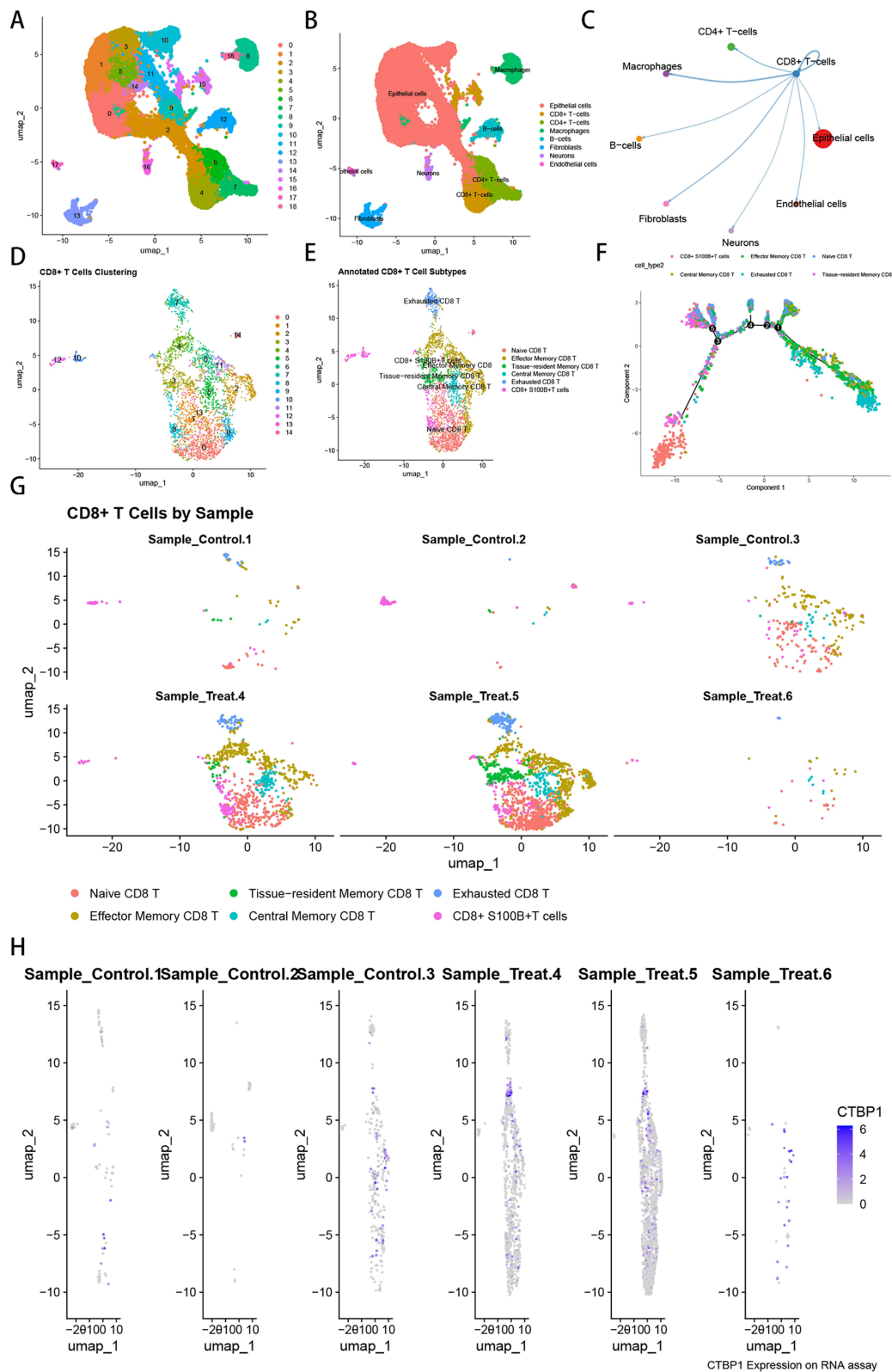


Figure 4 Identification of CD8+ T cell subpopulations and CTBP1 expression in breast cancer tissues. **(A)** UMAP of all 16 single-cell clusters from six breast tissue samples; **(B)** Same UMAP colored by major cell-type annotation (epithelial cells, CD8+ T cells, CD4+ T cells, macrophages, B cells, fibroblasts, neurons, endothelial cells); **(C)** CellChat communication probability heatmap; **(D)** UMAP of CD8+ T cell; **(E)** UMAP of reclustered CD8+ T cells, showing six subpopulations (Naive, Effector Memory, Tissue-resident Memory, Central Memory, Exhausted, CD8+ S100B+ T cells); **(F)** Sample-split UMAP showing the distribution differences of CD8+ S100B+ T cells between control and tumor samples. **(G)** Pseudo-temporal cell differentiation trajectory. **(H)** UMAP of each sample, showing the distribution of CD8+ T cell subpopulations. **(H)** UMAP of each sample, showing CTBP1 expression in CD8+ T cells.

CTBP1 is an NADH-dependent transcriptional co-repressor that plays a critical role in tumorigenesis by regulating cell proliferation, migration, and epithelial-to-mesenchymal transition (EMT).¹⁴ As a gene associated with succinylation, CTBP1 also influences cellular metabolism, gene expression, and signal transduction through the regulation of intracellular succinylation modifications.⁹ Recent studies have highlighted the complex role of CTBP1 in various cancers, particularly in breast cancer, where its expression level is closely associated with tumor initiation and progression.¹³

Several reports have highlighted CTBP1's impact on breast cancer biology. Zhao et al demonstrated that CTBP1–ZEB1 complexes repress SREBF2 to modulate cholesterol homeostasis and EMT,¹¹ while De Luca et al showed CTBP1 activation promotes tumor proliferation and metastasis under metabolic syndrome conditions.^{11,12}

Building on prior work, we systematically established CTBP1's causal links to breast cancer via two-sample MR and SMR, and validated these findings across survival cohorts, GTEx/TCGA transcriptomes, and clinical ELISA assays. Our findings also suggest that CTBP1 may regulate immune cell populations, particularly CD8+ S100B+ T cell subsets, thereby modulating the tumor immune microenvironment. This finding is consistent with the protective role of T cells in breast cancer, as previous research has shown that high density of tumor-infiltrating T cells correlates with better prognosis in breast cancer patients, particularly in HER2-positive and triple-negative breast cancer.²⁴

Moreover, our DCE-MRI radiomics demonstrated that CTBP1 expression correlates positively with HHH_gldm_LargeDependenceHighGrayLevelEmphasis ($r=0.28$, $p<0.05$) and negatively with HHH_gldm_SmallDependenceLowGrayLevelEmphasis ($r=-0.27$, $p<0.05$), emphasizing CTBP1's role in modulating tumor texture complexity and supporting its value as a noninvasive imaging biomarker.²⁵ In our study, higher CTBP1 expression was associated with tumor morphological complexity and texture homogeneity, suggesting that CTBP1 may play a protective role in the tumor, such as glioblastoma and²⁶ small cell lung cancer, where they were found to correlate with tumor texture and immune infiltration patterns.²⁷ By linking the molecular mechanisms of CTBP1 with MRI features, we gain a more comprehensive understanding of how CTBP1 functions as a protective factor in breast cancer. These imaging features, corresponding with molecular CTBP1 expression levels, provide visual evidence that CTBP1 may influence tumor invasiveness and metastatic potential.

Our single-cell analyses are limited by a modest sample size, and DCE-MRI associations require validation in larger, multi-center, multi-ethnic cohorts. Moreover, the molecular mechanisms underlying CTBP1's divergent roles in CD8+ S100B+ T cells remain to be elucidated through targeted *in vitro* and *in vivo* experiments.

Conclusion

CTBP1 appears to have context-dependent associations with breast cancer: inverse at the systemic (whole-blood) level yet nominally positive within a specific CD8+ S100B+ T-cell niche. Its expression shows modest correlations with DCE-MRI texture-dependence features. These observations prioritize CTBP1 for further study, though they should be interpreted cautiously. Validation in larger, multi-center cohorts and targeted mechanistic work will be essential to clarify biological pathways and its potential translational relevance.

Data Sharing Statement

The datasets used in this study were downloaded from the TCGA and GTEx databases. For further details regarding the datasets or additional requests, please contact the corresponding author (Keng Ling).

Ethics Approval and Consent to Participate

This research was approved by the ethics review board of the Jiaying Hospital of Traditional Chinese Medicine (Jiaying Medical Ethics Review 2023 Research No. 095-1), and all procedures were complied with the ethical principal of Helsinki Declaration. All the participants fully understood the goals and process of the research and provided the written informed consent. Clinical trial registration number: MR-33-23-052212.

Author Contributions

All authors made substantial contributions to all aspects of the work reported, including conception, study design, execution, acquisition of data, analysis, and interpretation, and were involved in drafting, revising, or critically reviewing

the article. All authors gave final approval of the version to be published and agree to be accountable for all aspects of the work.

Funding

The research was supported by the grants of Zhejiang Provincial Natural Science Foundation of China (Grant No. LQN25H180008), Medical Science and Technology Project of Zhejiang Province (Grant No. 2025KY366, 2024KY454, 2025KY1627), Public Welfare Research Project of Jiaxing (Grant No. 2024AY10026), and Zhejiang Traditional Chinese Medicine Administration (Grant No. 2024ZL1058).

Disclosure

The authors declare that they have no competing interests.

References

- Barrios CH. Global challenges in breast cancer detection and treatment. *Breast*. 2022;62(Suppl 1):S3–s6. doi:10.1016/j.breast.2022.02.003
- Hickey M, Basu P, Sassarini J, et al. Managing menopause after cancer. *Lancet*. 2024;403(10430):984–996. doi:10.1016/S0140-6736(23)02802-7
- Mubarik S, Yu Y, Wang F, et al. Epidemiological and sociodemographic transitions of female breast cancer incidence, death, case fatality and DALYs in 21 world regions and globally, from 1990 to 2017: an age-period-cohort analysis. *J Adv Res*. 2022;37:185–196. doi:10.1016/j.jare.2021.07.012
- Ni G, Sun Y, Jia H, et al. MAZ-mediated tumor progression and immune evasion in hormone receptor-positive breast cancer: targeting tumor microenvironment and PCLAF+ subtype-specific therapy. *Transl Oncol*. 2025;52:102280. doi:10.1016/j.tranon.2025.102280
- Wu Y, Shi Y, Luo Z, et al. Spatial multi-omics analysis of tumor-stroma boundary cell features for predicting breast cancer progression and therapy response. *Front Cell Develop Biol*. 2025;13:1570696. doi:10.3389/fcell.2025.1570696
- H LZ, Ma P, He Y, et al. The mechanism and latest progress of m6a methylation in the progression of pancreatic cancer. *Int J Bio Sci*. 2025;21(3):1187–1201. doi:10.7150/ijbs.104407
- Zou R, Jiang S, Mei J, et al. High-ammonia microenvironment promotes stemness and metastatic potential in hepatocellular carcinoma through metabolic reprogramming. *Discover Oncol*. 2025;16(1):182. doi:10.1007/s12672-025-01922-8
- Mu R, Ma Z, Lu C, et al. Role of succinylation modification in thyroid cancer and breast cancer. *Am J Cancer Res*. 2021;11(10):4683–4699.
- Zhao G, Zhen J, Liu X, et al. Protein post-translational modification by lysine succinylation: biochemistry, biological implications, and therapeutic opportunities. *Genes Dis*. 2023;10(4):1242–1262. doi:10.1016/j.gendis.2022.03.009
- Cheng X, Wang K, Zhao Y, et al. Research progress on post-translational modification of proteins and cardiovascular diseases. *Cell Death Discovery*. 2023;9(1):275. doi:10.1038/s41420-023-01560-5
- Zhao Z, Hao D, Wang L, et al. CtBP promotes metastasis of breast cancer through repressing cholesterol and activating TGF- β signaling. *Oncogene*. 2019;38(12):2076–2091. doi:10.1038/s41388-018-0570-z
- de Luca P, Dalton GN, Scalise GD, et al. CtBP1 associates metabolic syndrome and breast carcinogenesis targeting multiple miRNAs [J]. *Oncotarget*. 2016;7(14):18798–18811. doi:10.18632/oncotarget.7711
- Chen X, Zhang Q, Dang X, et al. The CtBP-CtBP1/2-HDAC1-API transcriptional complex is required for the transrepression of DNA damage modulators in the pathogenesis of osteosarcoma. *Transl Oncol*. 2022;21:101429. doi:10.1016/j.tranon.2022.101429
- Han Y, Bi Y, Bi H, et al. miR-137 suppresses the invasion and procedure of EMT of human breast cancer cell line MCF-7 through targeting CtBP1. *Human Cell*. 2016;29(1):30–36. doi:10.1007/s13577-015-0124-4
- Zhou J, Yan X, Liu Y, et al. Succinylation of CTBP1 mediated by KAT2A suppresses its inhibitory activity on the transcription of CDH1 to promote the progression of prostate cancer. *Biochem Biophys Res Commun*. 2023;650:9–16. doi:10.1016/j.bbrc.2023.02.002
- Hou X, Chen Y, Li X, et al. Protein succinylation: regulating metabolism and beyond. *Frontiers in Nutrition*. 2024;11:1336057. doi:10.3389/fnut.2024.1336057
- Shen R, Ruan H, Lin S, et al. Lysine succinylation, the metabolic bridge between cancer and immunity. *Genes Dis*. 2023;10(6):2470–2478. doi:10.1016/j.gendis.2022.10.028
- Kubatzky KF, Gao Y, Yu D. Post-translational modulation of cell signalling through protein succinylation. *Expl Targeted Anti-Tumor Ther*. 2023;4(6):1260–1285. doi:10.37349/etat.2023.00196
- Jézéquel P, Gouraud W, Ben Azzouz F, et al. bc-GenExMiner 4.5: new mining module computes breast cancer differential gene expression analyses. *Database*. 2021;2021:doi: 10.1093/database/baab007
- Posta M, Györfy B. Pathway-level mutational signatures predict breast cancer outcomes and reveal therapeutic targets. *Br J Pharmacol*. 2025;182:5734–5747. doi:10.1111/bph.70215
- M VDW, De Vries DH, Groot HE, et al. The single-cell eQTLGen consortium. *Elife*. 2020;9.
- Vösa U, Claringbould A, Westra HJ, et al. Large-scale cis- and trans-eQTL analyses identify thousands of genetic loci and polygenic scores that regulate blood gene expression. *Nat Genet*. 2021;53(9):1300–1310. doi:10.1038/s41588-021-00913-z
- Li H, Courtois ET, Sengupta D, et al. Reference component analysis of single-cell transcriptomes elucidates cellular heterogeneity in human colorectal tumors. *Nat Genet*. 2017;49(5):708–718. doi:10.1038/ng.3818
- Garaud S, Buisseret L, Solinas C, et al. Tumor infiltrating B-cells signal functional humoral immune responses in breast cancer. *JCI Insight*. 2019;5(18). doi:10.1172/jci.insight.129641.
- Hong M, Fan S, Xu Z, et al. MRI radiomics and biological correlations for predicting axillary lymph node burden in early-stage breast cancer. *J Transl Med*. 2024;22(1):826. doi:10.1186/s12967-024-05619-4

26. Gaebe K, Li AY, Park A, et al. Stereotactic radiosurgery versus whole brain radiotherapy in patients with intracranial metastatic disease and small-cell lung cancer: a systematic review and meta-analysis. *Lancet Oncol.* 2022;23(7):931–939. doi:10.1016/S1470-2045(22)00271-6
27. Lamichhane B, Lueckel PH, Dierker D, et al. Structural gray matter alterations in glioblastoma and high-grade glioma-A potential biomarker of survival. *Neurooncol Adv.* 2023;5(1):vdad034. doi:10.1093/noajnl/vdad034

Breast Cancer: Targets and Therapy

Publish your work in this journal

Breast Cancer - Targets and Therapy is an international, peer-reviewed open access journal focusing on breast cancer research, identification of therapeutic targets and the optimal use of preventative and integrated treatment interventions to achieve improved outcomes, enhanced survival and quality of life for the cancer patient. The manuscript management system is completely online and includes a very quick and fair peer-review system, which is all easy to use. Visit <http://www.dovepress.com/testimonials.php> to read real quotes from published authors.

Submit your manuscript here: <https://www.dovepress.com/breast-cancer—targets-and-therapy-journal>

Dovepress
Taylor & Francis Group